SARS-CoV-2 RNA elements share human sequence identity and upregulate hyaluronan via NamiRNA-enhancer network

Wei Li,[a,b,1] Shuai Yang,[a,b,1] Peng Xu,[a,b,1] Dapeng Zhang,[c,1] Ying Tong,[a,b,1] Lu Chen,[a,b,1] Ben Jia,[d] Ang Li,[e,h] Cheng Lian,[a,b] Daoping Ru,[a,b] Baolong Zhang,[a,b] Mengxing Liu,[a,b] Cancan Chen,[a,b] Weihui Fu,[e,h] Songhua Yuan,[e,h] Chenjian Gu,[f] Lu Wang,[g] Wenxuan Li,[a,b] Ying Liang,[a,b] Zhicong Yang,[a,b] Xiaoguang Ren,[a,b] Shaoxuan Wang,[a,b] Xiaoyan Zhang,[e,h] Yuanlin Song,[g] Youhua Xie,[f] Hongzhou Lu,[h] Jianqing Xu,[e,h]* Hailin Wang,[c]* and Wenqiang Yu [a,b]**

[a]Laboratory of RNA Epigenetics, Institutes of Biomedical Sciences & Shanghai Public Health Clinical Center & Department of General Surgery, Huashan Hospital, Cancer Metastasis Institute, Shanghai Medical College, Fudan University, Shanghai 200032, China
[b]Shanghai Key Laboratory of Medical Epigenetics, Shanghai 200032, China
[c]State Key Laboratory of Environmental Chemistry and Ecotoxicology, Research Center for Eco-Environmental Sciences, Chinese Academy of Sciences, Beijing 100085, China
[d]Shanghai Epiprobe Biotechnology Co., Ltd, Shanghai 200233, China
[e]Institute of Clinical Science & Shanghai Key Laboratory of Organ Transplantation, Zhongshan Hospital, Institutes of Biomedical Sciences, Shanghai Medical College, Fudan University, Shanghai 200032, China
[f]Key Laboratory of Medical Molecular Virology (MOE/NHC/CAMS), Department of Medical Microbiology and Parasitology, School of Basic Medical Sciences, Shanghai Medical College, Fudan University, Shanghai 200032, China
[g]Department of Pulmonary and Critical Care Medicine, Zhongshan Hospital, Fudan University, Shanghai 200032, China
[h]Shanghai Public Health Clinical Center, Fudan University, Shanghai 201508, China

Summary

Background Since late 2019, SARS-CoV-2 infection has resulted in COVID-19 accompanied by diverse clinical manifestations. However, the underlying mechanism of how SARS-CoV-2 interacts with host and develops multiple symptoms is largely unexplored.

Methods Bioinformatics analysis determined the sequence similarity between SARS-CoV-2 and human genomes. Diverse fragments of SARS-CoV-2 genome containing Human Identical Sequences (HIS) were cloned into the lentiviral vector. HEK293T, MRC5 and HUVEC were infected with laboratory-packaged lentivirus or transfected with plasmids or antagomirs for HIS. Quantitative RT-PCR and chromatin immunoprecipitation assay detected gene expression and H3K27ac enrichment, respectively. UV-Vis spectroscopy assessed the interaction between HIS and their target locus. Enzyme-linked immunosorbent assay evaluated the hyaluronan (HA) levels of culture supernatant and plasma of COVID-19 patients.

Findings Five short sequences (24−27 nt length) sharing identity between SARS-CoV-2 and human genome were identified. These RNA elements were highly conserved in primates. The genomic fragments containing HIS were predicted to form hairpin structures *in silico* similar to miRNA precursors. HIS may function through direct genomic interaction leading to activation of host enhancers, and upregulation of adjacent and distant genes, including cytokine genes and *hyaluronan synthase 2 (HAS2)*. HIS antagomirs and Cas13d-mediated HIS degradation reduced *HAS2* expression. Severe COVID-19 patients displayed decreased lymphocytes and elevated D-dimer, and C-reactive proteins, as well as increased plasma hyaluronan. Hymecromone inhibited hyaluronan production *in vitro*, and thus could be further investigated as a therapeutic option for preventing severe outcome in COVID-19 patients.

Interpretation HIS of SARS-CoV-2 could promote COVID-19 progression by upregulating hyaluronan, providing novel targets for treatment.

eBioMedicine 2022;76: 103861
Published online xxx
https://doi.org/10.1016/j.ebiom.2022.103861

*Corresponding authors.**Corresponding author at: Laboratory of RNA Epigenetics, Institutes of Biomedical Sciences & Shanghai Public Health Clinical Center & Department of General Surgery, Huashan Hospital, Cancer Metastasis Institute, Shanghai Medical College, Fudan University, Shanghai 200032, China.
E-mail addresses: xujianqing@shphc.org.cn (J. Xu), hlwang@rcees.ac.cn (H. Wang), wenqiangyu@fudan.edu.cn (W. Yu).
[1] These authors contributed equally to this work.

Funding The National Key R&D Program of China (2018YFC1005004), Major Special Projects of Basic Research of Shanghai Science and Technology Commission (18JC1411101), and the National Natural Science Foundation of China (31872814, 32000505).

Keywords: SARS-CoV-2; Human Identical Sequences; NamiRNA-enhancer network; Hyaluronan

Research in context

Evidence before this study

The coronavirus disease 2019 (COVID-19) pandemic caused by SARS-CoV-2 infection has swept across the world. Both DNA and RNA viruses can generate small RNAs to mediate the interaction between hosts and viruses. We previously discovered that a series of miRNA located in nucleus could activate gene expression by targeting enhancers, termed "Nuclear activating miRNAs (NamiRNAs)". Significantly, the transcripts of SARS-CoV-2 could be enriched in the host nucleolus. Except for the functional transcripts, SARS-CoV-2 can also produce numerous unknown transcripts. However, very little is known regarding how these unknown transcripts function in the interaction between host and SARS-CoV-2.

Add value of this study

We identified five short elements sharing sequence identity between SARS-CoV-2 and human genomes, at lengths of 24 nt to 27 nt, which we have named Human Identical Sequences (HIS). *In vitro*, HIS of SARS-CoV-2 activated expression of both adjacent and distant genes associated with inflammation by directly interacting with human enhancers. One of the activated genes, *hyaluronan synthase 2 (HAS2)* resulted in the accumulation of hyaluronan, which was closely correlated with the severity of COVID-19. HIS antagomirs and hyaluronan synthesis inhibitor 4-Methylumbelliferone (4-MU) inhibited the formation of hyaluronan, which could be an effective strategy for blocking the clinical progression of COVID-19.

Implications of all the evidence available

Our findings highlight that the interaction between HIS of SARS-CoV-2 and their target enhancers in human loci may contribute to COVID-19 progression by activating gene transcription. Hyaluronan may be a useful biomarker to predict the progression of COVID-19, and could be explored as a therapeutic target for COVID-19. The discovery of HIS expands our understanding of potential pathogeneses of viruses and contributes to the development of nucleic acid drugs for virus-related disease.

Introduction

The coronavirus disease 2019 (COVID-19) pandemic has resulted in more than 274 million identified cases and 5.3 million confirmed deaths worldwide as of 21 December, 2021 according to the WHO Coronavirus (COVID-19) Dashboard. COVID-19 is caused by severe acute respiratory syndrome coronavirus 2 (SARS-CoV-2) and clinically characterized by fever, dry cough, and shortness of breath.[1,2] Furthermore, COVID-19 may develop into acute liver and kidney injury, cardiac injury, bleeding, and coagulation dysfunction.[3] Severe patients frequently experience acute respiratory distress syndrome (ARDS), causing 70% of deaths in fatal cases.[4] Unfortunately, we still lack any specific strategies for treating COVID-19.

As a single-stranded positive-sense RNA virus, SARS-CoV-2 is closely related to other highly pathogenic beta-coronaviruses such as severe acute respiratory syndrome coronavirus (SARS-CoV) and Middle East respiratory syndrome coronavirus (MERS-CoV).[5] It has been revealed that SARS-CoV-2 enters the cell through the binding of spike (S) protein to angiotensin-converting enzyme 2 (ACE2) receptor.[6,7] SARS-CoV-2 infection activates both innate and adaptive immune responses,[8] accompanied by elevated inflammation markers (such as C-reactive protein (CRP), IL-2R, IL-6, IL-10, and TNF-α).[9] Noteworthily, as the antiviral immunity guardian, T cells are reduced significantly in COVID-19 patients,[10] which is negatively correlated with survival rates. In addition, the increased D-dimer concentration in COVID-19 patients remarkably suggests that SARS-CoV-2 infection activates the fibrinolytic system.[11] However, the molecular mechanisms underlying these clinical features caused by SARS-CoV-2 await further investigation.

Accumulating evidence has revealed an intriguing phenomenon that both DNA and RNA viruses can generate small RNAs different from that of the host cells in infected cells,[12–14] which are called virus-derived small RNAs (vsRNAs) or miRNA-like non-coding RNAs (v-miRNAs). For example, one of the vsRNAs derived from enterovirus 71 (EV71) inhibits viral translation and replication by targeting its internal ribosomal entry site (IRES).[15] Conversely, influenza A virus-generated vsRNAs promote virus RNA synthesis.[16] Other than

regulating virus replication, vsRNAs also function in regulating host response and disease processes. For instance, repression of LMP2A by miR-BART22 derived from the Epstein-Barr virus (EBV) protects the infected cells from host immune surveillance.[17] Moreover, vsRNAs can mediate the silencing of host genes in *Caenorhabditis elegans*,[18] and SARS-CoV virus N gene-derived small RNA (vsRNA-N) could enhance lung inflammatory pathology.[19] Recent research identified 7 key miRNAs in SARS-CoV-2 genomes, similar to human miRNAs.[20] However, little is known on whether SARS-CoV-2 derived vsRNAs participate in the replication of virus or the host response in COVID-19 patients.

MicroRNAs (miRNAs) are 19−23 nucleotides (nt) non-coding RNAs (ncRNAs) that primarily regulate post-transcriptional silencing by targeting the 3'-untranslated region (3'-UTR) of mRNA transcripts in the cytoplasm.[21] However, we discovered that miRNAs located in the nucleus were capable of activating gene expression by targeting enhancers and termed them as "Nuclear activating miRNAs (NamiRNAs)".[22,23] Consistent with our findings, Sharp and colleagues deciphered the interaction between super-enhancers (SEs) and miRNA networks.[24] NamiRNAs not only activate adjacent genes by targeting the enhancer where miRNA is located, but also activate distant genes by targeting other enhancers. SARS-CoV-2 was projected to be enriched in the nucleolus by a computational model named RNA-GPS.[25] Besides, numerous unknown transcripts have been identified from the architecture of SARS-CoV-2 transcriptome in infected Vero cells,[26] which may serve as precursor miRNAs (pre-miRNAs). Therefore, these findings imply that SARS-CoV-2 may generate vsRNAs that function in host cells.

Here we identified five sets of short sequences which share identity between SARS-CoV-2 and humans, which we refer to as "Human Identical Sequences (HIS)". They are conserved fragments with high similarity across different primates. Further bioinformatics analysis indicated that HIS embedded in SARS-CoV-2 could potentially encode virus-derived small RNAs. HIS-SARS-CoV-2 RNA could directly bind to their target human DNA loci *in vitro*. Moreover, these virus fragments containing HIS could increase enhancer marker H3K27 acetylation (H3K27ac) enrichment at the corresponding regions of the human genome in different mammalian cell lines and activate the expression of adjacent and distant genes associated with inflammation. Notably, HIS also activated *hyaluronan synthase 2* (*HAS2*) and increased the production of hyaluronan *in vitro*. Further studies demonstrated an upregulation of hyaluronan in severe COVID-19 patients' plasma, which correlated with the severity and clinical manifestations of COVID-19. Further studies are needed to determine whether hyaluronan contributes to disease severity. Hyaluronan inhibitor treatment downregulated the hyaluronan level and thus may be a potential therapeutic strategy for COVID-19 patients worthy of further investigation.

Methods

Ethics

We retrospectively analyzed 137 COVID-19 patients admitted to The Shanghai Public Health Clinical Center (SPHCC), which was approved by the SPHCC Ethics Committee (YJ-2020-S008-02, March 26 in 2020). All participants provided written informed consent for sample collection and subsequent analyses. All animal treatments were approved by the Animal Research Ethics Committee of Fudan University (202109009S, September 9 in 2021).

Cell cultures

Transformed human embryonic kidney cell HEK293T, and human fetal lung fibroblast cell MRC5 cells were cultured in DMEM/High glucose medium (HyClone, Cat# SH30243.01B) supplemented with 10% FBS (Gibco, Cat# 10270-106) and 1% Penicillin-Streptomycin solution (HyClone, Cat# SV30010). Human umbilical vein endothelial cells (HUVEC) were cultured in the commercial culture medium (AllCells, Cat# H-004). VERO C1008 (E6) (Cat# GNO17) and its culture medium MEM Complete Medium (Cat# SCSP-651), HEK293T (Cat# GNHu17), and MRC5 (Cat# GNHu41) were bought from The Cell Bank of Type Culture Collection of Chinese Academy of Sciences.

Clinical subjects

The COVID-19 patients in SPHCC were confirmed in strict accordance with the World Health Organization (WHO) diagnostic criteria. Based on the Diagnosis and Treatment Protocol for Novel Coronavirus Pneumonia (Trial Version 7) released by National Health Commission & State Administration of Traditional Chinese Medicine on March 3, 2020, COVID-19 patients with pneumonia were categorized as mild and severe based on the characteristic pneumonia features of chest CT. During the hospitalization of COVID-19 patients, they accepted necessary laboratory examinations and imaging examinations at any time according to their conditions, including lymphocyte count (137 patients), D-dimer (132 patients), and CRP (135 patients). Moreover, ELISA was performed to detect the hyaluronan level in their plasma at the same time points.

Mice and hyaluronan administration

Eight-week-old C57BL6/J mice were bought from the Animal Center of Jiesijie in Shanghai. All mice were fed in independent ventilated cages in 12:12-h light-dark cycle. They were randomly divided into two

groups (n = 5/group). Hyaluronan between 200 to 400 kDa was dissolved in 1 × PBS. After anesthetization, the solvent hyaluronan (60 mg/kg) was intratracheal to mice as the experiment group. Meanwhile, the mice were treated with 1 × PBS as the control group. The lungs of mice were monitored via micro CT imaging.

Viral genome and human genome blast & filter

The DNA BLAST was completed between the SARS-CoV-2 reference genome (Accession number: NC_045512) and the human reference genome (hg38) online (http://asia.ensembl.org/Multi/Tools/Blast) with the follow parameters:

(1) search against: Human and DNA database (Genome sequence); (2) search tool: BLASTN; (3) Search Sensitivity: normal; (4) General options: ① Maximum number of hits to report: 100; ② Maximum E-value for reported alignments: 10; ③ Word size for seeding alignments:11; (5) Scoring options: ①Match/Mismatch scores: 1,-3; ② Gap penalties: Opening: 2; (6) Filters and masking options: ① Filter low complexity: choose; ② Filter query sequences using Repeat Masker: choose; (7) Searching result Filter: the 100% similarity results and the length more than 20 bp were kept for further studies.

RNA secondary structure prediction

RNA secondary structure prediction was calculated by the minimum free energy algorithm (MEF),[27,28] which was proposed by Zuker based on the energy date of experiments. The base pairs and nucleotides in the RNA molecule are connected by hydrogen bonds. Free energy is defined by the energy consumed to broke the hydrogen bonds in different substructures of the RNA secondary structure. SARS-CoV-2 RNA sequence in FASTA form was put in the web (https://tanuki.ibisc.univ-evry.fr/evryrna/mirnafold/mirnafold_form) and analyzed as follows: (1) sliding window size 150; (2) minimum hairpin size:0; (3) maximal thermodynamic value of hairpins:0; (4) percentage of verified features:70; (5) species parameters: all miRBase.

Gene function annotation

Kyoto Encyclopedia of Genes and Genomes (KEGG) pathway and Gene Ontology (GO) analysis on the surrounding (±500 kb) genes of the identical sequences of HIS-SARS-CoV-2 in human genome and genes regulated by HIS-SARS2-CoV-2 via targeting pulmonary enhancer were performed using DAVID[29] and EnhancerAtlas 2.0.[30] GO biological processes were ranked by *P*-value.

Plasmid construction and antagomir synthesis

Five HIS in SARS-CoV-2 were chosen to construct plasmids, named HIS-SARS2-1, HIS-SARS2-2, HIS-SARS2-3, HIS-SARS2-4, and HIS-SARS2-5. Moreover, we chose HIS-SARS-1 in SARS-CoV as the parallel group. In brief, as HIS precursors, 100−150 bp virus DNA fragments containing 24−27 bp HIS in SARS-CoV and SARS-CoV-2 were obtained by annealing and extension with specific primers synthesized by Shanghai SunnyBio-technology Co., Ltd. Then, these HIS were cloned into the pCDH-CMV-MCS-EF1-copGFP lentiviral vector[31] at EcoR I (5') and BamH I (3') sites through ClonExpress II One Step Cloning Kit (Vazyme, Cat# C112) according to the manufacturer's manual. In addition, diverse single guide RNAs (sgRNAs) targeting the HIS precursors were designed and cloned into modified lentivirus plasmids containing Cas13d. Also, the antagomirs for HIS-SARS2-1, HIS-SARS2-2, HIS-SARS2-3, HIS-SARS2-4, HIS-SARS2-5, and HIS-SARS-1 were purchased from Guangzhou RiboBio Co., Ltd. The sequences of primers, HIS precursors, and antagomirs are listed in Table S1.

Vector transfection

Cells were transfected with plasmids or antagomirs at 70−80% confluency via Hieff Trans™ liposome nucleic acid transfection reagent (YEASEN, Cat# 40802ES02) following the manufacturer's instruction. We changed fresh medium containing 10% FBS at 6−8 h after transfection and harvested transfected cells at 72 h after transfection to detect the expression of HIS and target genes or perform ChIP assay. In addition, RNA sequencing was conducted to analyze the potential function of HIS using HEK293T cells transfected with the empty vector and HIS-SARS2-4 plasmid. The raw RNA-seq data reported in this paper have been deposited in the Genome Sequence Archive[32] in National Genomics Data Center,[33] China National Center for Bioinformation/Beijing Institute of Genomics, Chinese Academy of Sciences, under accession number HRA001589 that are publicly accessible at http://bigd.big.ac.cn/gsa-human.

Lentivirus package and cell screening

We co-transfected pCDH-pre-HIS, pSPAX2 (RRID: Addgene_12260), and pMD2.G (RRID: Addgene_12259) plasmids into HEK293T cells in a ratio of 4:3:1.2 and collected the virus supernatant by filtering cell culture supernatant with 0.45 μm filters at 48 h after changing the serum-containing medium. Then, cells were infected with different lentiviruses and cultured in medium with 1μg/ml puromycin to obtain stable cell lines.

SARS-CoV-2 viral RNA preparation

Vero cells were infected with SARS-CoV-2 strain nCoV-SH01 (GenBank: MT121215.1) at a multiplicity of

infection (MOI) of 0.05 and cultured in MEM complete medium at 37 °C, 5% CO_2 for 48 h; then we harvested cells to extract the total RNA. The study was approved by The Institutional Biosafety Committee of Shanghai Medical College Fudan University and experiments were perform in Biosafety Level 3 Laboratory at Shanghai Medical College, Fudan University.

Quantitative RT-PCR (RT-qPCR)

Total RNA was extracted from freshly harvested cells using TRIzol Reagent (Invitrogen, Cat# 10296028). Complementary DNA (cDNA) was synthesized with the PrimeScript™ RT reagent Kit (Takara, Cat# RR047A) involved in genomic DNA erasing. Quantitative PCR was performed using SYBR Green Pre-Mix (TIANGEN, Cat# FP205) on the Roche LightCycler480 instrument. *GAPDH* was the normalized endogenous control gene. Relative gene expression was calculated according to $2^{-\Delta Ct}$ method. The primers for target genes and diverse HIS precursor fragments are shown in Table S1.

Chromatin immunoprecipitation (ChIP)

ChIP assay was carried out as our previous study described.[22] In brief, transfected cells were cultured in 10 cm dishes and crosslinked with 1% formaldehyde in 1 × PBS for 10 min at room temperature. After sonication, sheared chromatin was immunoprecipitated with H3K27ac antibody (Abcam Cat# ab177178, RRID: AB_2828007) and Protein A magnetic beads (Invitrogen, Cat# 10002D) overnight at 4 °C. DNA from the chromatin immunocomplexes was extracted with QIAquick PCR Purification Kit (QIAGEN, Cat# 28106) according to the manufacturer's guidelines. ChIP-derived DNA was analyzed by quantitative PCR using SYBR Green PreMix (see Table S1 for primer sequences), and data were normalized by input DNA.

Loss-of-function assay for HIS

Loss-of-function of HIS was performed by inhibiting the enhancer components with JQ1 (Selleck Chemicals Inc., Cat# S7110) or blocking them via antagomirs synthesized by Guangzhou RiboBio Co., Ltd (see Table S1 for antagomir sequences). Cells were co-transfected with antagomirs and HIS precursor vectors and harvested at 72 h. Cells transfected with HIS precursor vectors were then treated with 500 nM JQ1 for 24 h. As indicated time points, total RNA was extracted from the harvested cells and the effect of loss-of-function for HIS on the target genes expression was evaluated by RT-qPCR.

UV-Vis spectroscopy measurement

UV-Vis spectroscopy experiments were performed on a SHIMADZU UV-1900 UV-Vis spectrophotometer (Tokyo, Japan) at room temperature. The DNA or/and RNA oligonucleotide, DNA-RNA hybrid, DNA duplex samples (2 mL) were diluted to 2.0 μM in 10 mM Tris-HCl, 50 mM NaCl buffer at pH 7.0. Spectra were recorded over a wavelength range from 350 to 200 nm with a scan rate at 100 nm/min and data interval for 1 nm. A 10 mm optical path length quartz cuvette was used for UV-Vis measurement.

Thermal melting (T_m) analysis

Melting temperatures (T_m) of self-complementary sequences were determined from the changes in absorbance at 260 nm as a function of temperature in a 10 mm path length quartz cuvette on a SHIMADZU UV-1900 UV-Vis spectrophotometer (Tokyo, Japan) equipped with a temperature control system. Solutions (2 mL) of 2 μM pre-hybridized DNA-RNA hybrid or DNA duplex in aqueous buffer (10 mM Tris-HCl, 50 mM NaCl, pH 7.5) were equilibrated at 10 °C for 5 min and then slowly ramped to 90 °C with 2 °C step at a rate of 1 °C/min. Tm values were calculated as the first derivatives of heating curves.

Probes preparation

All DNA-RNA hybrid and DNA duplex were prepared as follows: Firstly, the oligonucleotide was mixed with an equal molar of the complementary target strand in hybridization buffer (10 mM Tris-HCl pH 7.8, 50 mM NaCl, 1 mM EDTA), then the mixtures were annealed by heating them to 95 °C for 5 min, and then slowly cooled to room temperature. Secondly, the annealed mixtures were separated on 16% nondenaturing polyacrylamide gel at 100 V for 120 min using 0.5 × TBE as electrophoresis buffer. Thirdly, the target bands in the gel were cut and recovered the nucleic acid probes from the gel according to *Molecular Cloning: A Laboratory Manual*.[34]

Protein purification

Full-length hAGO2 coding sequence was amplified and cloned into the BamH I and Hind III restriction endonuclease sites of a home-reconstructed pMAL-C5X expression vector for protein purification. The constructed plasmid was transformed into a laboratory-built Dam knock out Rosetta (DE3) cells for protein expression. The colony was inoculated into 50 mL of LB containing 100 μg/mL ampicillin and allowed to grow overnight at 37 °C. This culture was diluted into 4L LB containing 100 μg/mL ampicillin and grown at 37 °C until A600 reached 0.4–0.6. Then the culture was overnight induced by the addition of 0.2 mM isopropyl-1-thio-β-D-galactopyranoside at 16 °C. The cells were harvested at 10,000 rpm for 5 min at 4 °C and then suspended in 100 mL lysis buffer (20 mM Tris-HCl pH 7.5, 500 mM NaCl, 10% glycerol, 1 mM DTT) supplemented with EDTA-free protease inhibitor. The

suspended cells were lysed by ultrahigh-pressure continuous flow cell breaker under the low-temperature (4 °C) water bath. Following centrifugation 12,000 rpm for 30 min at 4 °C, the cleared lysate was loaded onto 5 mL MBP Trap^{TM} HP column pre-equilibrated with 20 mM Tris-HCl pH 7.5, 200 mM NaCl, 10% glycerol, 0.2 mM DTT. The MBP-hAGO2 recombinant protein was eluted by the 20 mM Tris-HCl pH 7.5, 200 mM NaCl, 1.0 mM maltose, 10% glycerol, 0.2 mM DTT. The eluted recombinant protein was digested by thrombin to remove the MBP-tag under the ice-water bath, and then the digested mixture was further purified by the 1 mL His Trap HP column.

Electrophoretic mobility shift assay (EMSA)

The oligonucleotide probes (20 nM) were incubated with hAGO2 recombinant protein on the ice for 30 min in the fresh prepared binding buffer (10 mM PBS pH 7.5, 5 mM $MgCl_2$, and 0.1% Triton-100). The protein-substrate complexes were separated from the unbound substrate probes on 5% nondenaturing polyacrylamide gels at 100 V for 50 min using 0.5 × TBE as electrophoresis buffer. After electrophoresis, the resolved oligonucleotide probes in the gel were detected using an Odyssey CLx dual-color IR-excited fluorescence imaging system (LI-COR, Lincoln, NE).

Enzyme-linked immunosorbent assay (ELISA)

Hyaluronan of COVID-19 patients' plasma was measured in 1:5 dilution by the enzyme-linked sandwich assay Hyaluronan DuoSet ELISA (R&D Systems, Cat# DY3614-05, Minneapolis, MN, USA) following the manufacturer's descriptions. To evaluate the effect of hyaluronan inhibitor, 5×10^6 cells were seeded in 12-well plates and incubated for 24 h under appropriate treatments (with 500 μM 4-MU or 200 μg/ml hymecromone, and DMSO as the control group). Then, we collected the culture supernatants and quantified hyaluronan using the same ELISA kit. 4-MU (Cat# S2256) were purchased from Selleck. And hymecromone was provided from Correction Pharmaceutical Group Co., Ltd. in China.

Statistics

The mRNA relative expression level for each sample was evaluated by $2^{-\Delta Ct}$ method and presented relative to GAPDH. The results of RT-qPCR (Figs. 3a–i and 4), ChIP-qPCR (Fig. 3k) and hyaluronan detection of cell culture supernatants (Fig. 6a,g–h) are presented as mean ± SEM. *P*-values were calculated using the unpaired, two-tailed Student's *t* test by GraphPad Prism 7.0. The evaluation of clinical indicators of COVID-19 are shown in scatter plot (Fig. 6b–e), and the means were compared using the two-tailed nonparametric Mann–Whitney test by GraphPad Prism 7.0. *, $P < 0.05$; **, $P < 0.01$; ***, $P < 0.001$; ****, $P < 0.0001$; ns, not significant.

Role of the funding source

The funders had no role in study design, data collection, analysis and interpretation, writing and submission of the manuscript.

Results

Identification of human identical sequences in SARS-CoV-2 genome

Conserved regulatory elements have been revealed in certain viral genomes.[19,35] We previously identified a series of human miRNAs located in the nucleus, which could activate gene expression by interaction with enhancers.[22] Recent study showed that miR-339 can regulate tumor suppressor gene transcription by targeting enhancers in the human genome.[23] Therefore, we speculated that the interaction between nucleotide sequence of SARS-CoV-2 and human genome might function in SARS-CoV-2 infection and its pathogenicity during the clinical progression of COVID-19. Considering that the shortest regulatory RNAs are 19–23 nt miRNAs,[36] we first analyzed the sequence similarity between the genome of SARS-CoV-2 (accession number NC_045512) and human (GRCh38/hg38) with the following conditions: (1) length range of sequences are greater than 20 bp; (2) matching rate is 100%. Surprisingly, we found five fully identical sequences between the genome of SARS-CoV-2 and human (Fig. 1a), which were collectively termed as "Human Identical Sequences (HIS)". HIS-SARS-CoV-2-1 (abbreviated as "HIS-SARS2-1") and HIS-SARS2-2 are located in chromosome 3 (chr. 3) (Fig. 1b), while HIS-SARS2-3, HIS-SARS2-4, and HIS-SARS2-5 are in chromosome 5 (chr. 5), chromosome 18 (chr. 18), chromosome X (chr. X), respectively (Fig. S1a). HIS-SARS-CoV-2 were abbreviated as HIS-SARS2.

We further investigated the characteristics of these identical sequences of HIS-SARS2 in the human genome, and found that all these human genomic loci were widely associated with H3K27ac, a well-known marker of enhancers (Figs. 1c and S1b), suggesting that HIS-SARS2 may function as a regulator with the host enhancer. Intriguingly, there were many well-recognized genes near the location of HIS-SARS2 in human, including genes associated with inflammation (Fig. 1b). Furthermore, KEGG pathway analysis of the neighboring (±500 kb) genes of HIS showed that they were enriched in the cGMP-PKG signaling pathway and muscle contraction (Fig. 1d).

Collectively, we identified five HIS in the SARS-CoV-2 genome, and their targeted human genome loci were enriched with inflammation-related genes, indicating

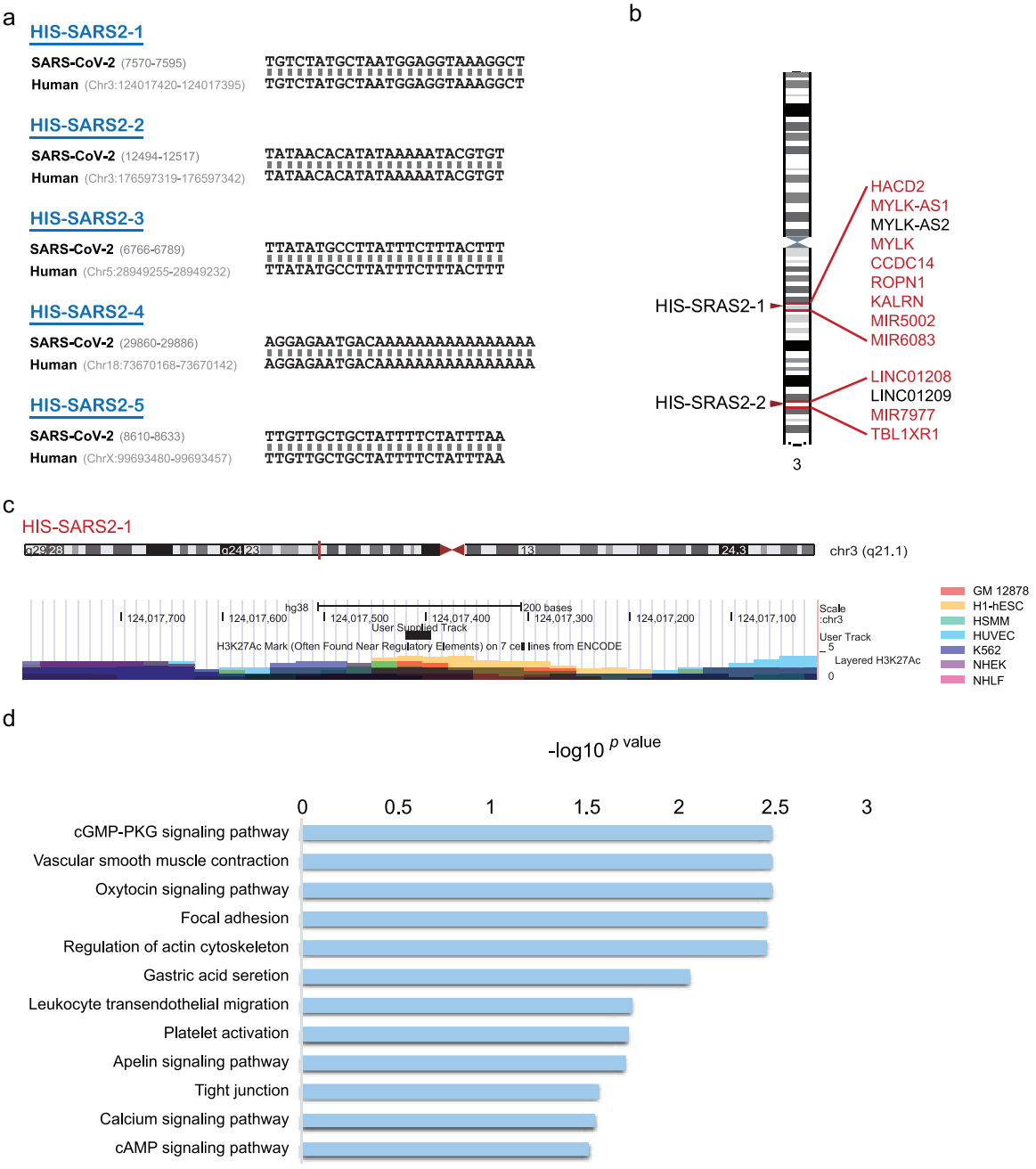

Figure 1. Identification of human identical sequences in SARS-CoV-2. (a) The sequences of five HIS identified in SARS-CoV-2. Numbers in parentheses indicate the location of HIS in the corresponding genomes. (b) The location of the identical sequence of HIS-SARS2-1 and HIS-SARS2-2 in human chromosome 3 and their surrounding genes. All genes within ± 500 kb of these loci are listed. Among them, inflammation- or immunity- related genes are written in red, which are defined by text mining (search combining keywords "gene name + inflammation" or "gene name + immunity") in PubMed and Google Scholar. (c) The distribution of enhancer marker H3K27 acetylation (H3K27ac) across the identical sequence of HIS-SARS2-1 in human genome in seven human cell lines. The location of the identical sequence of HIS-SARS2-1 is marked in red line and black block, respectively. (d) KEGG pathway enrichment analysis of genes within ± 500 kb of the identical sequences of HIS-SARS2 in human genomes.

that HIS may facilitate the inflammatory cytokine storm of COVID-19 patients and play a role in pathological progression.

Conservation and widespread of HIS

SARS-CoV-2 belongs to the *Coronavirinae* subfamily, which contains six well-known human coronaviruses

(HCoVs), including two alphacoronavirus (HCoV-299E, HCoV-NL63), two lineages A beta-coronavirus (HCoV-OC43, HCoV-HKU1), one lineage B beta-coronavirus (SARS-CoV), and one lineage C beta-coronavirus (MERS-CoV). To figure out whether HIS is a common feature embedded across the HCoVs' genome (The accession number for each HCoVs refers to Table S2), we analyzed the HCoVs and human genome sequence using the same criteria. Except for the five HIS in SARS-CoV-2 mentioned above, we identified 17 HIS overall, including five HIS in HCoV-HKU1, five HIS in HCoV-NL63, two HIS in HCoV-SARS, two HIS in HCoV-299E, two HIS in HCoV-OC43, and one HIS in MERS-CoV (Fig. 2a). Similar to HIS-SARS-CoV-2 being abbreviated as HIS-SARS2, HIS-SARS-CoV and HIS-MERS-CoV were abbreviated as HIS-SARS and HIS-MERS, respectively (The detailed information of 22 HIS in HCoVs refers to Table S3). Similarly, diverse sequences of HIS were embedded in the genome of other more than 100 pathogenic RNA viruses (Table S4), such as the Avian influenza virus, HIV, Ebolavirus, and Zika virus.

To explore the distribution of HIS-SARS2 across species, we explored the conversation of HIS in 19 different species, including eight primates (human, rhesus, crab-eating macaque, baboon, green monkey, marmoset, squirrel monkey, bushbaby), squirrel, mouse, rat, pig, cat, dog, four bats (megabat, David's myotis bat, microbat, big brown bat) and chicken (The accession number for each species refers to Table S2). Results demonstrated that all five HIS-SARS2 were highly conserved in primates (Figs. 2b and S2). Among them, HIS-SARS2-1, HIS-SARS2-4, and HIS-SARS2-5 were also highly conserved in bats and relatively poorly conserved in other mammals, such as squirrel, mouse, rat, cat, or dog (Figs. 2b and S2c,d); while HIS-SARS2-2 and HIS-SARS2-3 showed weakly conservation except primates (Fig. S2a,b). When it comes to the domesticated animals exampled by chicken, which is the main host for avian influenza, no conserved HIS were identified.

These results imply that the conservation of HIS across species may be a hint of the propagation evolution pathway of SARS-CoV-2, which highlights the potential significance of HIS.

HIS-SARS2 forms miRNA-like precursors

To investigate whether HIS can work as miRNAs, RNA secondary structures prediction[37] was performed to evaluate the potential of HIS-containing fragments in forming typical hairpin structures. HIS-containing fragments were predicted to form the typical hairpin structure like miRNA precursors (Figs. 2c and S3), suggesting that HIS are similar in structure and function to

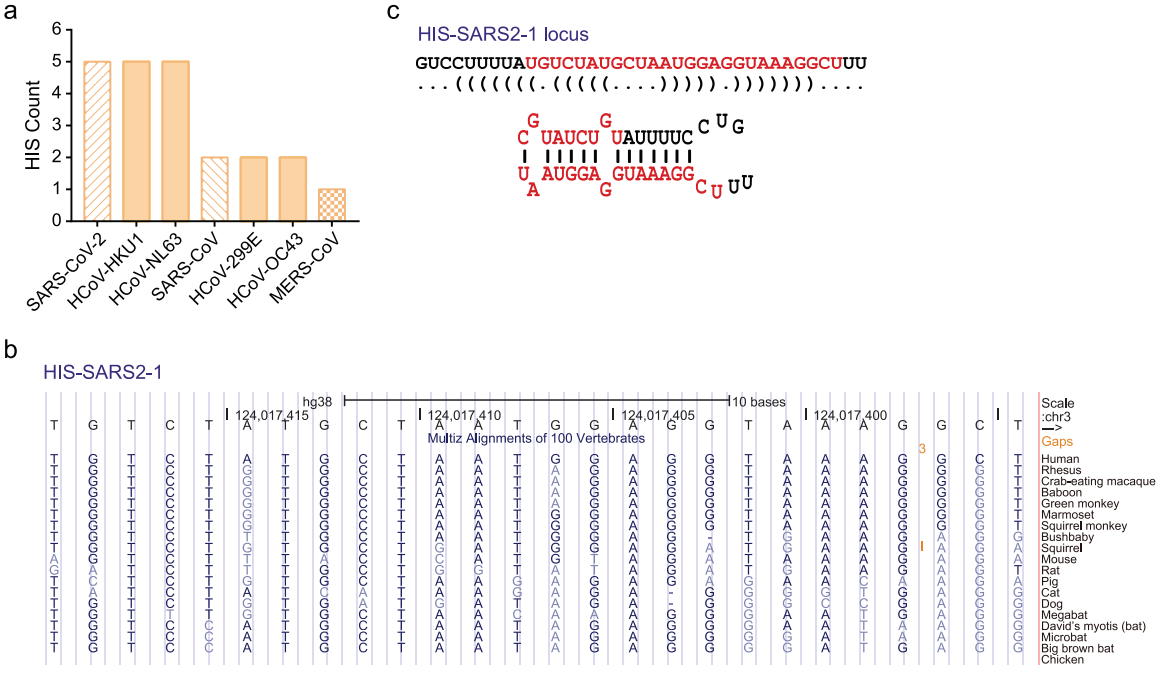

Figure 2. The distribution and conservation of HIS. (a) Number of HIS identified in seven known HCoVs. (b) The sequence conservation of HIS-SARS2-1 in 19 species. The color of bases represents the conservation degree, dark blue represents the fully conserved, while light blue represents the mismatched base, single line (-) indicates no bases in the aligned species. (c) The predicted RNA secondary structures of HIS-SARS2-1 and its adjunct bases (defined as pre-HIS-SARS2-1) by the algorithm of minimum free energy. The sequence in red represents HIS-SARS2-1 RNA.

miRNA. In addition, *in silico* prediction tools suggest that SARS-CoV-2 RNA could potentially be found in the host nucleolus[25], indicating that HIS-SARS2 may function in the nucleus. Combining these results above, we suspected that HIS-SARS2 could interact with host enhancers and function as NamiRNA.

HIS-SARS2 activates host genes involved in COVID-19 pathogenic processes

To investigate whether HIS could activate host gene expression, we constructed vectors containing HIS fragments from SARS-CoV-2 and SARS-CoV. We transfected them into HEK293T, MRC5, and HUVEC, and detected the expression of both surrounding and distant genes, which could be regulated through HIS and human enhancer interaction. The expression level of coronavirus fragments was verified by RT-qPCR (Fig. S4a–c). We confirmed that HIS precursor fragments were also detected in Vero cells with SARS-CoV-2 infection (Fig. S4d,e) and COVID-19 patients (Fig. S4f). HIS-SARS2-1 could upregulate the upstream gene *KALRN* in the HEK293T cell (Fig. S5a). KALRN contributes to the development of sarcoidosis,[38] a systemic inflammatory disease involved in multiple organs throughout the body. Likely, *FBXO15, TIMM21*, and *CYB5A* were localized upstream of the targeted locus of HIS-SARS2-4. As an E3 ligase subunit, FBXO15 impairs mitochondrial integrity and induces lung injury in pneumonia.[39] Both *TIMM21* and *CYB5A* encode the components of mitochondrial membrane,[40,41] implying their fundamental roles in mitochondria. Simultaneously, we found *FBXO15* was upregulated when HIS-SARS2-4 was transfected into HEK293T (Fig. 3a), MRC5 (Fig. 3b), and HUVEC (Fig. 3c). Meanwhile, *TIMM21* and *CYB5A* were upregulated in HEK293T (Fig. 3a) and MRC5 (Fig. 3b), respectively. Besides, HIS can also work as cis-regulatory elements. For example, *MYL9* was obviously up-regulated by HIS-SARS2-3 in HEK293T (Fig. 3d) and MRC5 (Fig. 3e). MYL9 was demonstrated to be a functional ligand for CD69 that regulates airway inflammation.[42] And the same results of *EPN1* were found in MRC5 (Fig. 3e) and HUVEC (Fig. 3f). EPN1 could facilitate atherogenesis through recruiting proinflammatory macrophage.[43]

Furthermore, HIS-SARS-1 could also activate neighboring gene expression, such as *HAS2*, and *ZHX2*in HEK293T (Fig. S5b), MRC5 (Fig. S5c), and HUVEC (Fig. S5d). Importantly, *HAS2* encodes the critical enzyme for the production of hyaluronan, which accumulates in the lung of ARDS patients infected with SARS-CoV.[44] Given that ARDS is the most typical clinical manifestation of severe COVID-19 cases,[1,45] it is intriguing to explore whether HIS-SARS2 could activate *HAS2*. Surprisingly, we found that both HIS-SARS2-3 and HIS-SARS2-4 could activate the expression of *HAS2* about 2–4 folds in HEK293T (Fig. 3g) and MRC5 (Fig. 3h). Remarkably, the expression of *HAS2* was upregulated more than ten folds in HUVEC (Fig. 3i). In addition, we noticed that ACE2 was also upregulated by HIS-SARS2-3 and HIS-SARS2-4 (Fig. S5e). Accordingly, the expression of HAS2 and ACE2 was significantly activated in SARS-CoV-2 infected Vero cells (Fig. S5f).

Combined with the enhancer database EnhancerAtlas 2.0,[30] we also identified the target genes regulated by the pulmonary specific enhancers and HIS-SARS2 regulatory cascade. Interestingly, the lung's enhancers which are targeted by HIS could regulate 298 genes (Table S5) supported by recent results made by the bronchoalveolar lavage fluid (BALF) of COVID-19 patients transcriptome sequencing.[46] Importantly, 58 of all genes regulated by HIS-SARS2 were involved in the "cytokine activity term" (GO:0005125) (Table S6), such as IL-6, CXCL10, and CCL2, which were increased significantly in COVID-19 patients.[46,47] Additionally, we performed functional annotation of all genes regulated by HIS-SARS2 in lung. As shown in Fig. S6a, these genes were significantly enriched in cell-cell adhesion, apoptotic process, viral process, mRNA splicing via spliceosome, which was also supported by the findings that SARS-CoV-2 infection indeed disrupts the mRNA splicing, protein translation and trafficking in host cells.[48] Moreover, we performed RNA sequencing to evaluate the functional consequence of the HIS-mediated gene activation in HEK293T cells. Given that HIS could activate gene expression by targeting enhancer, functional annotation was carried out from the upregulated genes (Fig. S6b). Notably, viral process was also enriched in the upregulated genes caused by HIS-SARS2-4. At the same time, cilium assembly and cilium morphogenesis were surprisingly observed in the functional annotation of differentially expressed genes of SARS-CoV-2–infected ciliated cells in COVID-19 patients.[49] Consistent with this finding, the infection of SARS-CoV-2 caused the ultrastructurally abnormal cilia of the ciliated cells.[50] In accordance with DNA repair, the DNA damage response was triggered by SARS-CoV-2 in Vero E6 cells.[51]

Therefore, these results demonstrate that HIS-SARS2 can activate adjacent and distant host genes, which have been previously implicated to be involved in COVID-19 pathogenesis.

HIS-SARS2 activates the host genes through NamiRNA-enhancer network

H3K27ac marks enhancers , which is critical for gene activation. To explore the underlying mechanism of HIS-SARS2 regulated gene expression, we transfected HEK293T with HIS fragments and performed H3K27ac ChIP-qPCR. We found that HIS fragments could increase the enrichment of H3K27ac at HIS targeted loci (Fig. 3k). JQ1, as a potent inhibitor of the BET family proteins, could inhibit gene expression regulated by

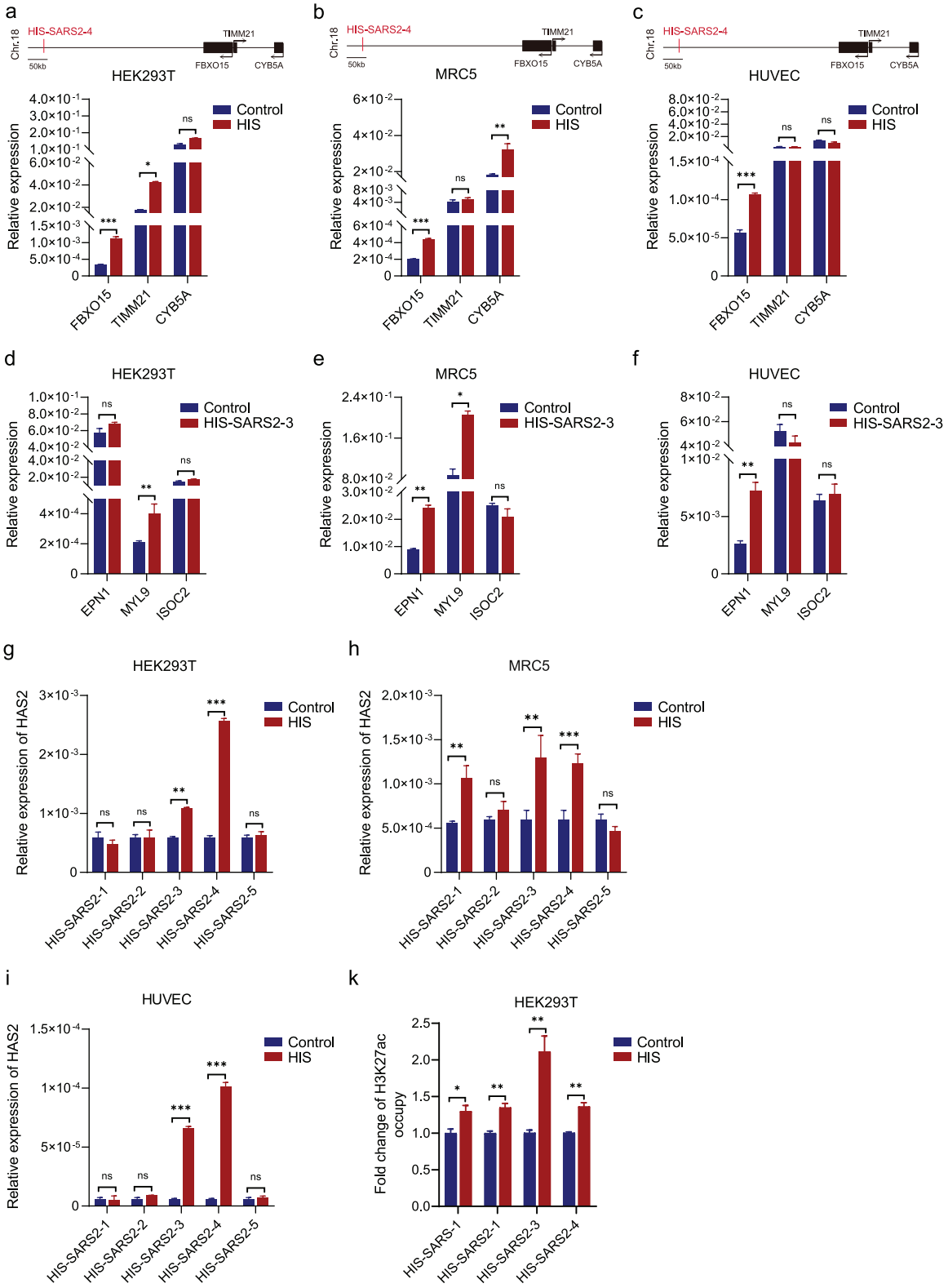

Figure 3. HIS-SARS2 activates genes related to COVID-19 pathology. (a–c) The relative mRNA expression of the neighboring genes *FBXO15*, *TIMM21*, and *CYB5A* after HIS-SARS2-4 vector transfected in HEK293T cells (a), MRC5 cells (b), and HUVEC cells (c). (d–f) The

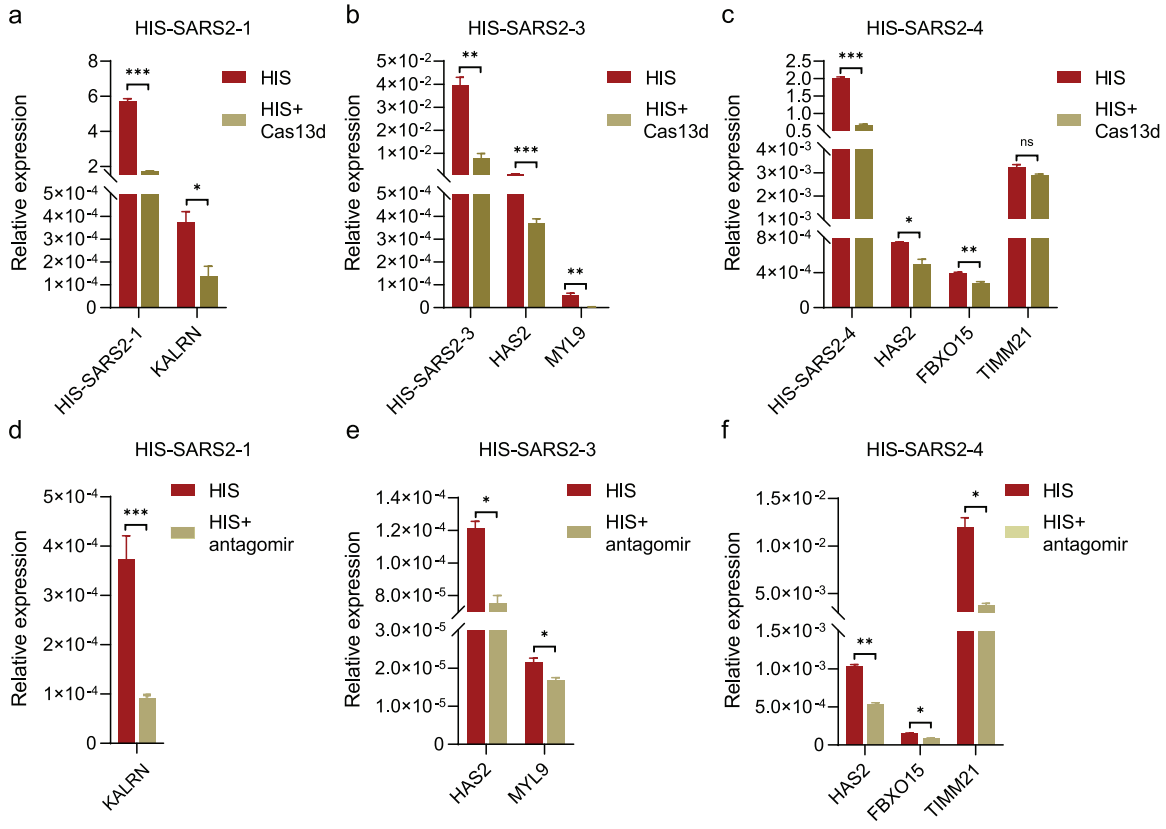

Figure 4. Loss-of-function of HIS abolishes the upregulation of their targeted genes. (a) The relative mRNA expression of HIS-SARS2-1 targeted gene *KALRN* in HEK293T cells after Cas13d knocked down HIS-SARS2-1. (b) The relative mRNA expression of HIS-SARS2-3 targeted genes *HAS2* and *MYL9* in HEK293T cells after Cas13d knocked down HIS-SARS2-3. (c) The relative mRNA expression of HIS-SARS2-4 targeted genes *HAS2, FBXO15*, and *TIMM21* in HEK293T cells after Cas13d knocked down HIS-SARS2-4. (d–f) The relative mRNA expression of the targeted gene *KALRN* (d), *MYL9* (e), *HAS2, FBXO15*, and *TIMM21* (f) after transfection of antagomirs of HIS-SARS2-1, HIS-SARS2-3, and HIS-SARS2-4, respectively. Data are represented as mean ± SEM ($n = 3$). In all figures, *P*-values were calculated using the unpaired, two-tailed Student's *t* test by GraphPad Prism 7.0. *, $P < 0.05$; **, $P < 0.01$; ***, $P < 0.001$; ns, not significant.

enhancers. And we found that the upregulation of HIS targeted genes (such as *KALRN, HAS2*, and *MYL9*) was abolished after JQ1 treatment (Fig. S7). To further confirm whether HIS is indispensable for gene activation, we knocked down HIS expression by Cas13d and found that the activation of targeted genes was abolished (Fig. 4a–c). Moreover, we transfected cells with HIS antagomirs and found that antagomirs of HIS-SARS2-1, HIS-SARS2-3, and HIS-SARS2-4 downregulated the corresponding inflammatory genes, such as *KALRN* (Fig. 4d), *HAS2, MYL9* (Fig. 4e), *FBXO15*, and *TIMM21* (Fig. 4f). These data revealed the specificity of HIS for regulating the host genes, which suggest that targeting HIS may be an efficient strategy for fighting against RNA virus-related disease. The behaviors of HIS-SARS2 RNA are highly similar to our earlier identified NamiRNAs, which activate genes as enhancer triggers in the nucleus.[22,52] Overall, these data suggest that HIS activate the host gene through the NamiRNA-enhancer network.

HIS-SARS2 RNA binds to identical human DNA stabilized by AGO2

To confirm the binding between HIS and its targeted sequences in the human genome, we synthesized HIS-SARS2 and their target DNA fragments (Table S1). We detected the interaction between HIS-SARS2-1 and its

relative mRNA expression of the distant gene *EPN1, MYL9*, and *ISOC2* after HIS-SARS2-3 vector transfected in HEK293T cells (d), MRC5 cells (e), and HUVEC cells (f). (g–i) The relative mRNA expression of HSA2 after five HIS-SARS2 vectors transfected in HEK293T cells, MRC5 cells, and HUVEC cells. (k) The enrichment of enhancer marker H3K27ac after HIS-SARS-1, HIS-SARS2-1, HIS-SARS2-3, and HIS-SARS2-4 transfection. Data are represented as mean ± SEM ($n = 3$). *P*-values were calculated using the unpaired, two-tailed Student's *t* test by GraphPad Prism 7.0. *, $P < 0.05$; **, $P < 0.01$; ***, $P < 0.001$; ns, not significant.

target DNA by UV absorption spectra. Generally, after the hybridization, the absorbance of the hybrid strand will decrease. When HIS-SARS2-1 RNA and its target ssDNA (HIS-SARS2-1 DNA-S, S represents sense strand) were hybridized, the absorbance significantly decreased compared with the theoretically calculated and mixed (before hybridization) group, indicating that HIS-SARS2-1 could hybridize its target DNA and form double strands (Fig. 5a). Comparing to the relative absorbance change, we found that when 50% product dissociated, the corresponding T_m value for HIS-SARS2-1-RNA-DNA hybrid (62.7 °C) was higher than dsDNA (60.3 °C) (Fig. 5b), which reflected the robustness of the HIS-SARS2-1-RNA-DNA hybrid over dsDNA.

Previously, we have shown that AGO2 was also essential for the NamiRNA-enhancer-gene activation cascade.[53] Here, we investigated whether AGO2 was necessary for HIS-induced gene activation. We assessed the interaction between human AGO2 (hAGO2) and HIS-SARS2-1 DNA-S, HIS-SARS2-1 dsDNA, HIS-SARS2-1 RNA-DNA-Hybrid by EMSA assay. It showed that hAGO2 could partially bind to HIS-SARS2-1 DNA-S in high hAGO2 concentrations (Fig. 5c), while the interaction between hAGO2 and HIS-SARS2-1 dsDNA or the HIS-SARS2-1 RNA-DNA-Hybrid was more intense (Fig. 5d,e), which was verified in a fixed concentration of hAGO2 (Fig. 5f). We simulated the hAGO2 binding curves of these three forms of nucleic acid and calculated the corresponding dissociation constant (K_d). Results demonstrated that the HIS-SARS2-1 RNA-DNA-Hybrid has the smallest K_d, indicating the strongest binding ability. Compared with the HIS-SARS2-1 RNA-DNA-Hybrid, HIS-SARS2-1 dsDNA exhibited a relatively low binding capability, and HIS-SARS2-1 DNA-S bound weakly to hAGO2 (Fig. 5g).

These data suggest that HIS-SARS2 RNAs could bind to their targeted DNA loci in the host genome, which further support that HIS-SARS2 can potentially activate genes related to COVID-19 pathology via the AGO2-dependent NamiRNA-enhancer network.

Hyaluronan acts as a predictor of progression and therapeutic target for COVID-19 treatment

ARDS is one of the common clinical symptoms of SARS-CoV and SARS-CoV-2 infected patients. It has been proven that hyaluronan accumulates in the lung of patients with adult respiratory distress syndrome.[44] Among HIS-activated genes, *HAS2* arose to our special attention for its ability to regulate hyaluronan levels. Along with the upregulation of *HAS2* activated by HIS-SARS-1, HIS-SARS2-3, and HIS-SARS2-4, we found that HIS significantly upregulated the hyaluronan level in supernatant of culture medium for HEK293T (Fig. 6a), which was also the case for MRC5 (Fig. S8a).

To examine whether hyaluronan may play a role in COVID-19 disease, we collected the plasma from COVID-19 patients who have been hospitalized at The Shanghai Public Health Clinical Center. We categorized patients into mild (n = 37) and severe (n = 100) groups based on the characteristic pneumonia features of chest CT. In severe patients, the mean value of hyaluronan (80.39 ng/mL) (Fig. 6b) was significantly ($P < 0.0001$) higher than that in mild patients (5.70 ng/mL), suggesting that hyaluronan may act as a predictor of COVID-19 severity.

In order to test whether hyaluronan itself could be an indicator for characterizing the clinical manifestations of COVID-19 patients, we categorized patients into mild and severe groups based on their hyaluronan levels. We found that in severe patients, the level of lymphocytes decreased (Fig. 6c), D-Dimer increased (Fig. 6d), and CRP was significantly elevated (Fig. 6e), which were in line with reported indicators of severity in COVID-19 patients[54]. Ground-glass opacity (GGO) of lung is another typical clinical symptom in COVID-19 patients,[55] which can develop into consolidation. We further reproduced this pathogenic progression in mice, and results showed that pulmonary lesions, including GGO and consolidation were induced by hyaluronan administration (Fig. 6f). These data suggest that hyaluronan may contribute to COVID-19 severity.

For the purpose of further testing whether hyaluronan could function as a target for COVID-19 progression, we treated HEK293T with 4-Methylumbelliferone (4-MU), a hyaluronan synthesis inhibitor[56]. After treatment, hyaluronan was downregulated in all groups (Fig. 6g), which was also the case for MRC5 (Fig. S8b). We noted that hymecromone was an oral prescription drug containing 4-MU. Similarly, we treated HEK293T with DMSO-dissolved hymecromone and found that hyaluronan levels reduced accordingly in the cell culture supernatants (Fig. 6h).

Taken together, hyaluronan promoted by HIS may emerge as a potential target for COVID-19 treatment, and the downregulation of *HAS2* by HIS antagomirs or blocking hyaluronan synthesis by hymecromone may provide novel strategies for treating COVID-19 patients by blocking progression from developing severity.

Discussion

It is critical to understand the mechanisms of how SARS-CoV-2 causes inflammation leading to cytokine storm in the host. In this current study, we observed that HIS-SARS2 activate host genes associated with inflammation through the NamiRNA-enhancer network. Ectopic expression of these fragments containing HIS-SARS2 promotes H3K27ac enrichment at their corresponding enhancer regions in host cells. It is notable that these HIS-SARS2 can bind to their targeting loci

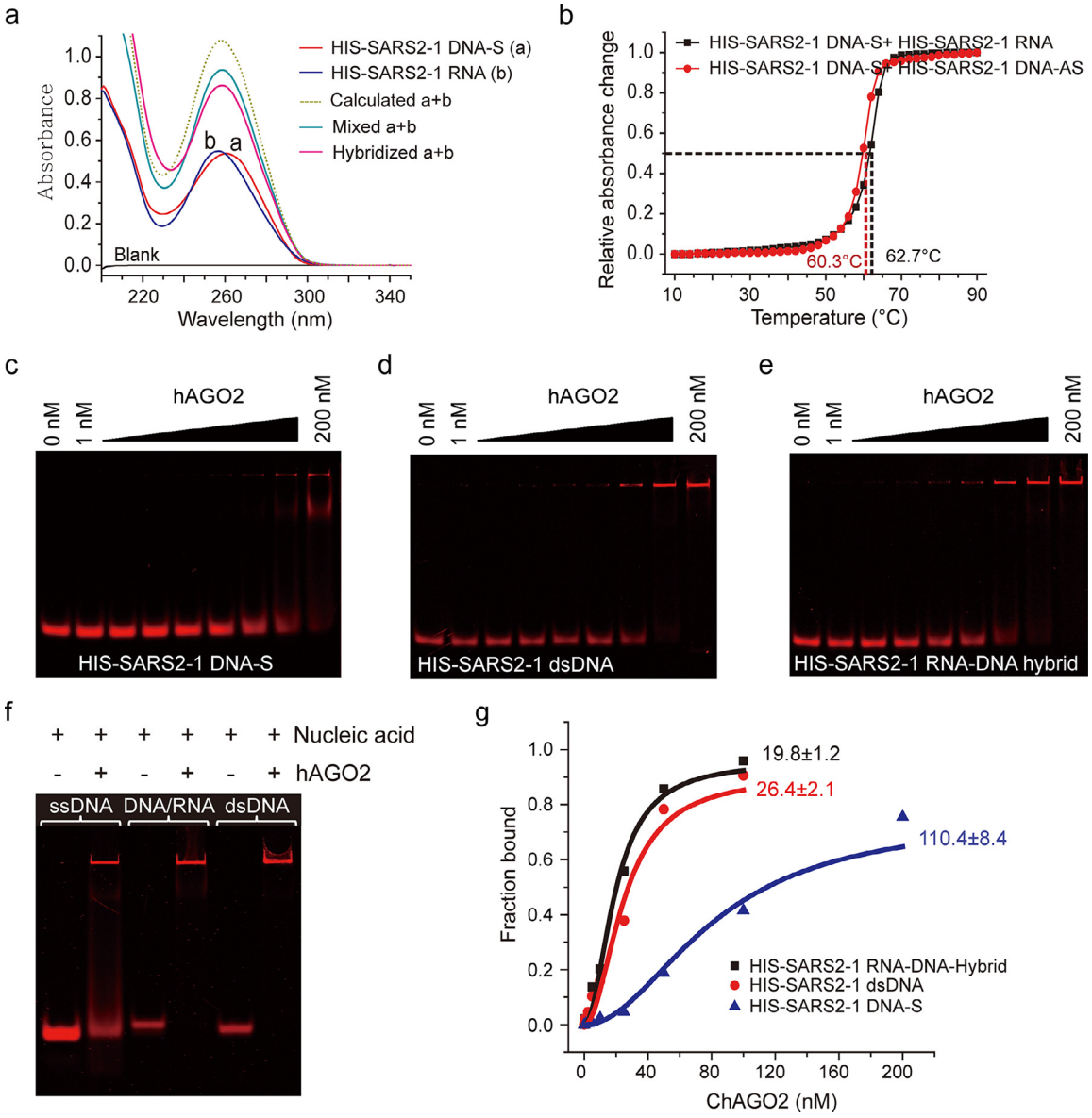

Figure 5. HIS-SARS2 RNA binds to homologous sequence of human genome for gene activation. (a) The UV absorption spectra of 2 μM HIS-SARS2-1 DNA (red curve a), 2 μM HIS-SARS2-1 RNA (blue curve b), mixed HIS-SARS2-1 DNA and RNA (dark cyan curve), hybridized mixture of HIS-SARS2-1 (magenta curve), and the simple sum of curve a and b (dark yellow dotted curve). (b) The relative absorbance changes of 2 μM hybridized mixture of HIS-SARS2-1 and the complementary RNA-HIS-SARS2-1(black square) or HIS-SARS2-1 and the complementary ssDNA (red circle) at 260 nm versus temperature. (c) Gel showing of 25 nM 5′Cy5-HIS-SARS2-1 in the presence of increasing concentrations of hAGO2. (d) Gel showing of 25 nM 5′Cy5-HIS-SARS2-1 DNA duplex in the presence of increasing concentrations of hAGO2. (e) Gel showing of 25 nM 5′Cy5-HIS-SARS2-1 DNA-RNA hybrid in the presence of increasing concentrations of hAGO2. (f) Gel showing 25 nM 5′Cy5-HIS-SARS2-1 (lane 1, 2), 5′Cy5-HIS-SARS2-1 DNA-RNA hybrid (lane 3, 4), 5′Cy5-HIS-SARS2-1 DNA duplex (lane 5, 6) in the absence and presence of 100 nM hAGO2. (g) The bound fraction of 5′Cy5-HIS-SARS2-1 (blue triangle), 5′Cy5-HIS-SARS2-1 DNA-RNA hybrid (black square) and 5′Cy5-HIS-SARS2-1 DNA duplex (red circle) probes in the presence of different concentration of hAGO2.

within human genome facilitated by AGO2 *in vitro*. Importantly, HIS activates *HAS2* expression and increase hyaluronan level in different cells, while COVID-19 patients who have higher plasma hyaluronan levels were associated with severe symptoms. These results uncover potential pathogenic mechanisms underlying COVID-19 progression and provide novel therapeutic targets for COVID-19.

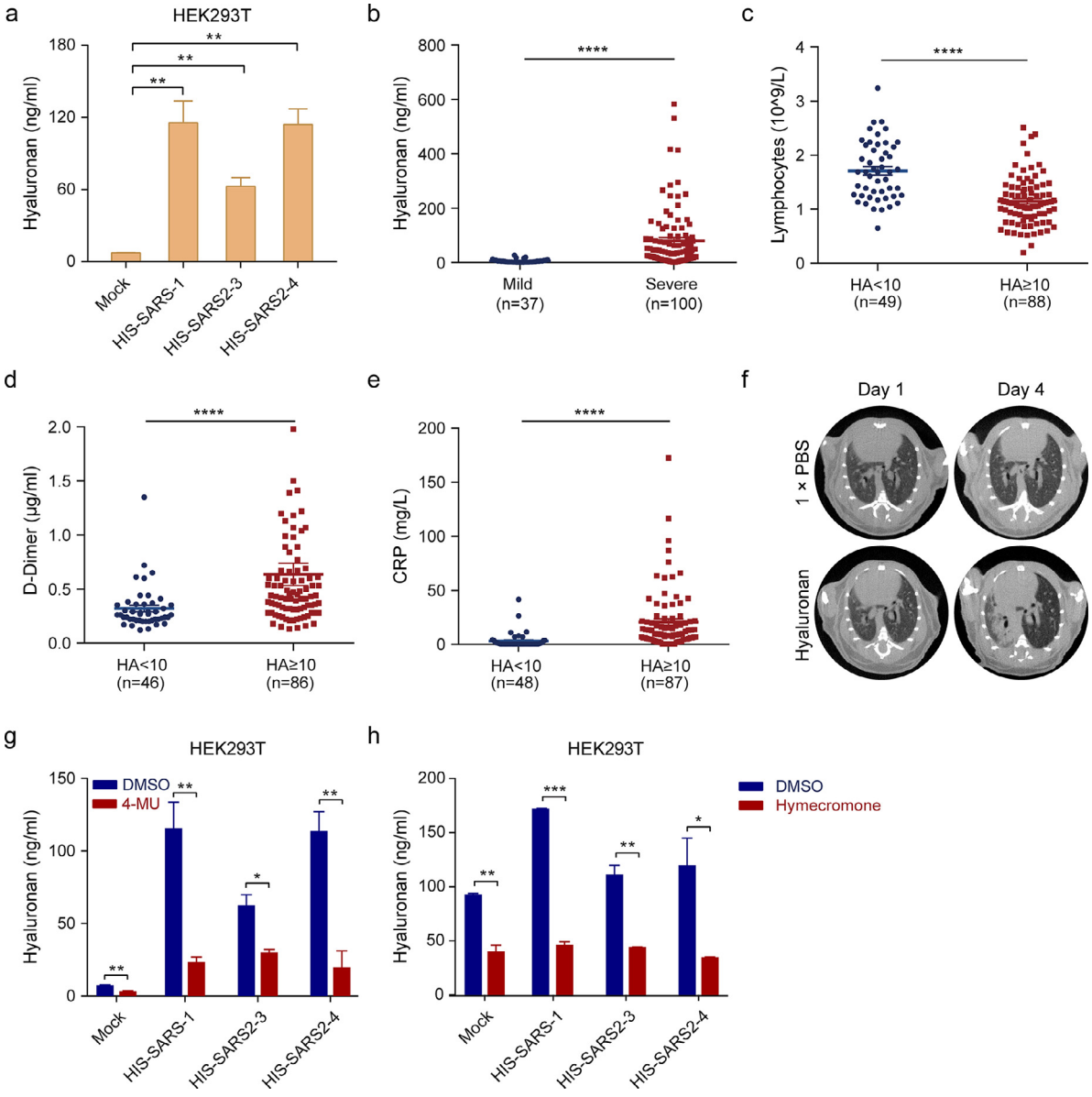

Figure 6. Hyaluronan can serve as a potential therapeutic target for COVID-19. (a) Hyaluronan released in cell culture supernatants of Mock, HIS-SARS-1, HIS-SARS2-3, and HIS-SARS2-4 overexpressed in HEK293T cell. (b) Hyaluronan in mild patients (n = 37) and severe patients (n = 100). (c-e) HA level (10 ng/mL) functions as a discriminator for patients' lymphocytes number (c), D-Dimer level (d), and CRP level (e). (f) Represented CT images of pulmonary lesions in mice treated with hyaluronan were presented (n = 5 / group). (g) HA released in cell culture supernatants of Mock, HIS-SARS-1, HIS-SARS2-3, or HIS-SARS2-4 overexpressed in HEK293T after treated with 500 μM 4-MU and DMSO as control. (h) HA released in cell culture supernatants of Mock, HIS-SARS-1, HIS-SARS2-3, and HIS-SARS2-4 overexpressed in HEK293T after treated with 200 μg/ml hymecromone and DMSO as control. Data are represented as mean ± SEM (n = 3). In (a, g-h), P-values were calculated using the unpaired, two-tailed Student's t-test; in (b−e), P-values were calculated using the two-tailed nonparametric Mann−Whitney test by GraphPad Prism 7.0. *, $P < 0.05$; **, $P < 0.01$; ***, $P < 0.001$; ****, $P < 0.0001$.

A growing number of studies indicate that the infection of various viruses, including both DNA and RNA viruses, has species- and organ-specific signatures.[57–60] We found HIS fragments are conserved in primates. We also identified HIS between other highly pathogenic beta-coronaviruses (such as SARS-CoV and MERS-CoV) and humans. In particular, HIS was found within other more than 100 pathogenic RNA viruses, including HIV,[61] Ebolavirus,[62] and Zika virus,[63] indicating a common phenomenon that pathogenic viruses share

identical genomic sequences to their hosts. Accordingly, these identical sequences, termed here as "host identical sequences (HIS)". There are also similar sequences between the genomes of SARS-CoV-2 and their potential hosts including bat,[64] Malayan pangolins,[65,66] ferrets, and cats.[67] Meanwhile there are no identical sequences between SARS-CoV-2 and chicken. In this case, it is natural to speculate that HIS from the pathogen genome may help to trace the lines of the host, especially for mediated hosts during SARS-CoV-2 virus evolution. Interestingly, SARS-CoV-2 infection in human results in COVID-19 without being fatal for its other potential hosts, including bats and pangolins,[6,66] which may be associated with different gene-network regulated by HIS targeted enhancers in diverse species. Therefore, HIS may be essential in viral susceptibility and pathogenicity.

Our results showed that HIS-SARS2 activate host genes associated with inflammation in the pathogenic processes. In recent years, multiple DNA and RNA viruses have been demonstrated to produce miRNA-like non-coding RNAs.[14] Previously, we revealed that miRNA located in the nucleus can activate tumor suppressor gene expression.[23] The fragments containing HIS in SARS-CoV-2 are predicted to form potential pre-miRNA structure, indicating HIS may function as miRNA-like RNAs. Further bioinformatic analysis showed that many HIS-SARS2 and enhancers cascade regulating genes are associated with cytokines, which may in part explain why most severe COVID-19 patients are characterized clinically by a cytokine storm, the main cause for ARDS leading to death.[68] Consistent with our KEGG pathway analysis for the genes regulated by HIS, modulation of cGMP-PKG pathway with the inhibitor of its upstream regulator phosphodiesterase 5 (PDE5) could be a potential treatment for COVID-19 patients.[69] An increasing number of research points to SARS-CoV-2 infection as causing multiple organ damage involved in the lung, kidney, and liver by activating the inflammation response.[3] Consistent with these findings, different HIS-SARS2 can upregulate genes associated with inflammation among HEK293T, MRC5, and HUVEC cells. For example, *KALRN* upregulated by HIS-SARS2-1 could cause systemic inflammation in multiple organs such as kidney and lungs.[38] Alternatively, HIS-SARS2 activates genes associated with mitochondria, such as *FBXO15*, *CYB5A*, and *TIMM21*, which may result in the mitochondrial dysfunction in COVID-19 pathogenesis.[70] Collectively, these evidence emphasize HIS-SARS2 probably as a potential key player of the inflammation response observed in COVID-19 through activation of gene expression.

We found that interaction between HIS-SARS2 and host enhancers activates host gene expression. MiRNAs can activate gene transcription epigenetically by triggering H3K27ac enrichment at their target enhancer regions.[22] Interestingly, H3K27ac was enriched in the corresponding DNA loci of the human genome that contains the identical sequences of HIS in HEK293T. Inhibition of enhancer function with JQ1 significantly reduced the gene activation (such as *FBXO15*) mediated by HIS-SARS2 in HEK293T, which further supports the notion that HIS-SARS2 mediated gene activation may be related to enhancer function. Furthermore, blocking HIS-SARS2 with antagomirs or degrading HIS-SARS2 with CasRx system significantly inhibited the gene upregulation (such as *FBXO15*) activated by HIS-SARS2, proving HIS-SARS2's indispensability in gene activation. During this process, AGO2 may serve as a guide mediating the binding of miRNAs to their target enhancers, resulting in gene activation.[53] Clearly, HIS-SARS2-4 RNA could hybridize its target ssDNA and form stable double strands, which can be stabilized by hAGO2 through reducing the dissociation constant (K_d). This implies that AGO2 may participate in the host gene activation due to HIS-SARS2. Therefore, these results demonstrate that HIS can activate gene transcription epigenetically by targeting enhancers mediated by AGO2. Given that HIS activate host genes through enhancers, which are well known for their tissue-specific signature, our findings may help unravel why viruses typically show organ or tissue-specific pathogenesis.

Importantly, we identified that hyaluronan could be a potential candidate target for COVID-19 treatment, once this is tested in human trials. At first, *HAS2* located upstream of the HIS targeted site in the human genome attracted our interest as the major enzyme responsible for hyaluronan synthesis.[71] HIS-SARS2 can activate *HAS2* expression drastically in host cells, causing the upregulation of hyaluronan in cell medium supernatant. Correspondingly, we found that hyaluronan is significantly increased in severe COVID-19 patients with ground-glass opacity by chest CT scan compared to the patients without GGO, and the level of hyaluronan is correlated with the clinical prognosis of patients with COVID-19.[72] Hyaluronan can absorb a large volume of water, which enables it to determine the water content in specific tissues.[73] It has been reported that the extravascular lung water volume is positively correlated with hyaluronan level in normal animal lungs.[74] Therefore, the water absorption characteristics of hyaluronan suggest the possibility that the increased hyaluronan induced by the upregulated *HAS2* in lung cells after SARS-CoV-2 infection, binds a large quantity of water and thereby forms the jelly-like substances underlying ground-glass opacity commonly observed in COVID-19 patients. Notably, hyaluronan directly causes GGO and consolidation of lung in mice, indicating that hyaluronan could be fundamental for the formation of GGO. The decreased lymphocytes, increased D-Dimer, and CRP observed in severe patients can be distinguished by their hyaluronan levels,

which is in surprising unanimity with the pathological features of ICU COVID-19 patients.[45] In other words, hyaluronan could be a potential indicator for characterizing the clinical progression of COVID-19 patients. Conspicuously, the total number of T cells was significantly reduced in COVID-19 patients compared to normal levels.[75] Such decrease of T cells may be due to the binding between hyaluronan and its ligand CD44, which can induce the death of activated T cells.[76] Another hyaluronan ligand HABP2 (also called factor VII-activating protease), which combines with hyaluronan, plays an important role in blood coagulation by activating the pro-urokinase-type plasminogen activator,[77] thereby causing the dysregulation of the fibrinolytic system in COVID-19 patients. In addition, HABP2 aggravates the disruption of the hyaluronan-mediated endothelial cell barrier,[78] which may help explain the sudden brain hemorrhage of ICU patients with COVID-19.[79] Further studies will need to be performed to elucidate the mechanisms behind hyaluronan's proposed links with these clinical characteristics of COVID-19 progression. 4-MU is reported to be an efficient inhibitor for hyaluronan production.[56] Our results demonstrate that 4-MU or hymecromone treatment can inhibit hyaluronan synthesis and block the pathogenic progression induced by HIS-SARS2. Overall, decreasing hyaluronan levels could be an efficient strategy for improving some clinical symptoms observed in COVID-19 patients.

There are some potential limitations in our study. It should be noted that the potential of hymecromone to prevent severe outcome in COVID-19 patients need to be tested in human trials in the future. Although SARS-CoV-2 replication generally occurs in the cytoplasm,[80] Burke and colleagues showed that part of SARS-CoV-2 mRNAs are located in nucleus,[81] which provides a glimpse that HIS could be located in nucleus. The location of HIS in nucleus need further to be confirmed in SARS-CoV-2 infected cells. Besides, hyaluronan is related to diabetes and hypertension,[82,83] the common complications for COVID-19, which need further investigate their potential relation in clinical trials.

Our *in vitro* results provide a potential mechanism whereby SARS-CoV-2 can induce the host response by regulating host gene expression through a direct interaction between HIS and their targeted enhancers following SARS-CoV-2 infection. This mechanism deepens our insights into the potential pathogenicity of diverse viruses. Our findings suggest that blocking HIS with nucleic acid drugs or inhibiting hyaluronan production with specific medication like hymecromone may provide new strategies for COVID-19 treatment.

Declaration of interests

Wenqiang Yu, Wei Li, Jianqing Xu, Hailin Wang, Cheng Lian, Peng Xu, Shuai Yang, and Daoping Ru are listed as inventors on patents' application related to this work; no other relationships or activities that could appear to have influenced the submitted work.

Contributors

W.Y. conceived this project. W.Y., H.W., J.X. took charge of the project administration. W.L., B.J., W.L., S. W. performed bioinformatic analysis. S.Y., Y.T., L.C., C. L., D.Z., D.R., B.Z., M.L., C.C., P.X., C.G., L.W., Y.L., Z. Y., X.R., Y.S., Y.X. performed experiments and analyzed data. A.L., W.F., S.Y., X.Z., H.L. coordinated patient enrollment and sample collection. W.L., S.Y., Y.T., L.C, C.L., C.C, W.Y. have verified the underlying data. P.X., S.Y. wrote the original draft. S.Y., W.L., P.X., W.Y., H. W., J.X. conducted critically review and editing of the manuscript. All authors read and approved the final version of the manuscript.

Acknowledgements

Modified Cas13d plasmid was a generous gift from Professor Pengyu Huang at ShanghaiTech University. We thank Yue Yu for editorial help and comments on the manuscript. We thank all the participants involved in this study. This research was supported by the National Key R&D Program of China (2018YFC1005004), Major Special Projects of Basic Research of Shanghai Science and Technology Commission (18JC1411101), and the National Natural Science Foundation of China (31872814, 32000505).

Data sharing statement

The raw sequence data reported in this paper have been deposited in GSA database (HRA001589) that are publicly accessible at https://ngdc.cncb.ac.cn/gsa. The other data are provided as figures, supplementary figures, or supplementary tables. Further information and requests for resources and reagents should be directed to and will be fulfilled by the Lead Contact, Wenqiang Yu (wenqiangyu@fudan.edu.cn).

Supplementary materials

Supplementary material associated with this article can be found in the online version at doi:10.1016/j.ebiom.2022.103861.

References

1 Guan WJ, Ni ZY, Hu Y, et al. Clinical characteristics of coronavirus disease 2019 in China. *N Engl J Med*. 2020;382(18):1708–1720.
2 Mao R, Qiu Y, He JS, et al. Manifestations and prognosis of gastrointestinal and liver involvement in patients with COVID-19: a systematic review and meta-analysis. *Lancet Gastroenterol Hepatol*. 2020;5(7):667–678.
3 Wiersinga WJ, Rhodes A, Cheng AC, Peacock SJ, Prescott HC. Pathophysiology, transmission, diagnosis, and treatment of

coronavirus disease 2019 (COVID-19): a review. *JAMA*. 2020;324 (8):782–793.
4 Zhang B, Zhou X, Qiu Y, et al. Clinical characteristics of 82 cases of death from COVID-19. *PLoS One*. 2020;15:(7) e0235458.
5 Hassan AO, Case JB, Winkler ES, et al. A SARS-CoV-2 infection model in mice demonstrates protection by neutralizing antibodies. *Cell*. 2020;182(3):744-53 e4.
6 Zhou P, Yang XL, Wang XG, et al. A pneumonia outbreak associated with a new coronavirus of probable bat origin. *Nature*. 2020;579(7798):270–273.
7 Hoffmann M, Kleine-Weber H, Schroeder S, Krüger N, Herrler T, Erichsen S, et al. SARS-CoV-2 cell entry depends on ACE2 and TMPRSS2 and is blocked by a clinically proven protease inhibitor. *Cell*. 2020;181(2):271. 80.e8.
8 Blanco-Melo D, Nilsson-Payant BE, Liu WC, et al. Imbalanced host response to SARS-CoV-2 drives development of COVID-19. *Cell*. 2020;181(5):1036-45 e9.
9 Chen G, Wu D, Guo W, et al. Clinical and immunological features of severe and moderate coronavirus disease 2019. *J Clin Invest*. 2020;130(5):2620–2629.
10 Diao BW, Tan C, Chen Y, et al. Reduction and functional exhaustion of T cells in patients with coronavirus disease 2019 (COVID-19). *Front Immunol*. 2020;11:827.
11 Levi M, Thachil J, Iba T, Levy JH. Coagulation abnormalities and thrombosis in patients with COVID-19. *Lancet Haematol*. 2020;7 (6):e438–ee40.
12 Weng KF, Hsieh PT, Huang HI, Shih SR. Mammalian RNA virus-derived small RNA: biogenesis and functional activity. *Microbes Infect*. 2015;17(8):557–563.
13 Shapiro JS. Processing of virus-derived cytoplasmic primary-microRNAs. *Wiley Interdiscip Rev RNA*. 2013;4(4):463–471.
14 Mishra R, Kumar A, Ingle H, Kumar H. The interplay between viral-derived miRNAs and host immunity during infection. *Front Immunol*. 2019;10:3079.
15 Weng KF, Hung CT, Hsieh PT, et al. A cytoplasmic RNA virus generates functional viral small RNAs and regulates viral IRES activity in mammalian cells. *Nucleic Acids Res*. 2014;42(20):12789–12805.
16 Perez JT, Varble A, Sachidanandam R, et al. Influenza A virus-generated small RNAs regulate the switch from transcription to replication. *Proc Natl Acad Sci U S A*. 2010;107(25):11525–11530.
17 Lung RW, Tong JH, To KF. Emerging roles of small Epstein-Barr virus derived non-coding RNAs in epithelial malignancy. *Int J Mol Sci*. 2013;14(9):17378–17409.
18 Guo X, Li WX, Lu R. Silencing of host genes directed by virus-derived short interfering RNAs in caenorhabditis elegans. *J Virol*. 2012;86(21):11645–11653.
19 Morales L, Oliveros JC, Fernandez-Delgado R, tenOever BR, Enjuanes L, Sola I. SARS-CoV-encoded small RNAs contribute to infection-associated lung pathology. *Cell Host Microbe*. 2017;21 (3):344–355.
20 Arisan ED, Dart A, Grant GH, et al. The prediction of miRNAs in SARS-CoV-2 genomes: hsa-miR databases identify 7 key miRs linked to host responses and virus pathogenicity-related KEGG pathways significant for comorbidities. *Viruses*. 2020;12(6).
21 Pasquinelli AE. MicroRNAs and their targets: recognition, regulation and an emerging reciprocal relationship. *Nat Rev Genet*. 2012;13(4):271–282.
22 Xiao M, Li J, Li W, et al. MicroRNAs activate gene transcription epigenetically as an enhancer trigger. *RNA Biol*. 2017;14(10):1326–1334.
23 Liang Y, Lu Q, Li W, et al. Reactivation of tumour suppressor in breast cancer by enhancer switching through NamiRNA network. *Nucleic Acids Res*. 2021;49(15):8556–8572.
24 Suzuki HI, Young RA, Sharp PA. Super-enhancer-mediated RNA processing revealed by integrative MicroRNA network analysis. *Cell*. 2017;168(6):1000–1014. e15.
25 Wu KE, Fazal FM, Parker KR, Zou J, Chang HY. RNA-GPS predicts SARS-CoV-2 RNA residency to host mitochondria and nucleolus. *Cell Syst*. 2020;11(1):102. 8.e3.
26 Kim D, Lee JY, Yang JS, Kim JW, Kim VN, Chang H. The architecture of SARS-CoV-2 transcriptome. *Cell*. 2020;181(4):914-21 e10.
27 Chen Y, Ye W, Zhang Y, Xu Y. High speed BLASTN: an accelerated MegaBLAST search tool. *Nucleic Acids Res*. 2015;43(16):7762–7768.
28 Bernhart SH, Hofacker IL, Will S, Gruber AR, Stadler PF. RNAalifold: improved consensus structure prediction for RNA alignments. *BMC Bioinf*. 2008;9:474.
29 Huang da W, Sherman BT, Lempicki RA. Systematic and integrative analysis of large gene lists using DAVID bioinformatics resources. *Nat Protoc*. 2009;4(1):44–57.
30 Gao T, Qian J. EnhancerAtlas 2.0: an updated resource with enhancer annotation in 586 tissue/cell types across nine species. *Nucleic Acids Res*. 2020;48(D1):D58–D64.
31 Zou Q, Xiao X, Liang Y, et al. miR-19a-mediated downregulation of RhoB inhibits the dephosphorylation of AKT1 and induces osteosarcoma cell metastasis. *Cancer Lett*. 2018;428:147–159.
32 Chen T, Chen X, Zhang S, et al. The genome sequence archive family: toward explosive data growth and diverse data types. *Genom Proteom Bioinform*. 2021. In press.
33 Members C-N, Partners. Database resources of the national genomics data center, China national center for bioinformation in 2021. *Nucleic Acids Res*. 2021;49(D1):D18–D28.
34 Green MR, Hughes H, Sambrook J, MacCallum P. Molecular cloning: a laboratory manual. *Molecular Cloning: A Laboratory Manual*. Cold Spring Harbor Laboratory Press; 2012:1890.
35 Bernard HU. Regulatory elements in the viral genome. *Virology*. 2013;445(1-2):197–204.
36 Fan PC, Chen CC, Chen YC, Chang YS, Chu PH. MicroRNAs in acute kidney injury. *Hum Genom*. 2016;10(1):29.
37 Mathews DH, Disney MD, Childs JL, Schroeder SJ, Zuker M, Turner DH. Incorporating chemical modification constraints into a dynamic programming algorithm for prediction of RNA secondary structure. *Proc Natl Acad Sci U S A*. 2004;101(19):7287–7292.
38 Besnard V, Calender A, Bouvry D, et al. G908R NOD2 variant in a family with sarcoidosis. *Respir Res*. 2018;19(1):44.
39 Chen BB, Coon TA, Glasser JR, et al. E3 ligase subunit Fbxo15 and PINK1 kinase regulate cardiolipin synthase 1 stability and mitochondrial function in pneumonia. *Cell Rep*. 2014;7(2):476–487.
40 Mick DU, Dennerlein S, Wiese H, et al. MITRAC links mitochondrial protein translocation to respiratory-chain assembly and translational regulation. *Cell*. 2012;151(7):1528–1541.
41 Plitzko B, Ott G, Reichmann D, et al. The involvement of mitochondrial amidoxime reducing components 1 and 2 and mitochondrial cytochrome b5 in N-reductive metabolism in human cells. *J Biol Chem*. 2013;288(28):20228–20237.
42 Hayashizaki K, Kimura MY, Tokoyoda K, et al. Myosin light chains 9 and 12 are functional ligands for CD69 that regulate airway inflammation. *Sci Immunol*. 2016;1(3):eaaf9154.
43 Brophy ML, Dong Y, Tao H, et al. Myeloid-specific deletion of epsins 1 and 2 reduces atherosclerosis by preventing LRP-1 downregulation. *Circ Res*. 2019;124(4):e6–e19.
44 Hällgren R, Samuelsson T, Laurent TC, Modig J. Accumulation of hyaluronan (hyaluronic acid) in the lung in adult respiratory distress syndrome. *Am Rev Respir Dis*. 1989;139(3):682–687.
45 Wu C, Chen X, Cai Y, et al. Risk factors associated with acute respiratory distress syndrome and death in patients with coronavirus disease 2019 pneumonia in Wuhan, China. *JAMA Intern Med*. 2020;180(7):934–943.
46 Xiong Y, Liu Y, Cao L, et al. Transcriptomic characteristics of bronchoalveolar lavage fluid and peripheral blood mononuclear cells in COVID-19 patients. *Emerg Microbes Infect*. 2020;9(1):761–770.
47 Zhang X, Tan Y, Ling Y, et al. Viral and host factors related to the clinical outcome of COVID-19. *Nature*. 2020;583(7816):437–440.
48 Banerjee AK, Blanco MR, Bruce EA, et al. SARS-CoV-2 disrupts splicing, translation, and protein trafficking to suppress host defenses. *Cell*. 2020;183(5):1325–1339. e21.
49 Ravindra NG, Alfajaro MM, Gasque V, et al. Single-cell longitudinal analysis of SARS-CoV-2 infection in human airway epithelium identifies target cells, alterations in gene expression, and cell state changes. *PLoS Biol*. 2021;19:(3) e3001143.
50 Robinot R, Hubert M, de Melo GD, et al. SARS-CoV-2 infection induces the dedifferentiation of multiciliated cells and impairs mucociliary clearance. *Nat Commun*. 2021;12(1):4354.
51 Victor J, Deutsch J, Whitaker A, et al. SARS-CoV-2 triggers DNA damage response in Vero E6 cells. *Biochem Biophys Res Commun*. 2021;579:141–145.
52 Zou Q, Liang Y, Luo H, Yu W. miRNA-mediated RNAa by targeting enhancers. *Adv Exp Med Biol*. 2017;983:113–125.
53 Liang Y, Xu P, Zou Q, Luo H, Yu W. An epigenetic perspective on tumorigenesis: loss of cell identity, enhancer switching, and NamiRNA network. *Semin Cancer Biol*. 2019;57:1–9.
54 Wang D, Li R, Wang J, et al. Correlation analysis between disease severity and clinical and biochemical characteristics of 143 cases of COVID-19 in Wuhan, China: a descriptive study. *BMC Infect Dis*. 2020;20(1):519.
55 Xie X, Zhong Z, Zhao W, Zheng C, Wang F, Liu J. Chest CT for typical coronavirus disease 2019 (COVID-19) pneumonia: relationship to negative RT-PCR testing. *Radiology*. 2020;296(2):E41–EE5.

56 Nagy N, Kuipers HF, Frymoyer AR, et al. 4-methylumbelliferone treatment and hyaluronan inhibition as a therapeutic strategy in inflammation, autoimmunity, and cancer. *Front Immunol*. 2015;6:123.
57 Rothenburg S, Brennan G. Species-specific host-virus interactions: implications for viral host range and virulence. *Trends Microbiol*. 2020;28(1):46–56.
58 De Meyer S, Gong ZJ, Suwandhi W, van Pelt J, Soumillion A, Yap SH. Organ and species specificity of hepatitis B virus (HBV) infection: a review of literature with a special reference to preferential attachment of HBV to human hepatocytes. *J Viral Hepat*. 1997;4 (3):145–153.
59 Iwamoto T, Okinaka Y, Mise K, et al. Identification of host-specificity determinants in betanodaviruses by using reassortants between striped jack nervous necrosis virus and sevenband grouper nervous necrosis virus. *J Virol*. 2004;78(3):1256–1262.
60 Ohlund P, Lunden H, Blomstrom AL. Insect-specific virus evolution and potential effects on vector competence. *Virus Genes*. 2019;55(2):127–137.
61 Levy JA. *HIV and the pathogenesis of AIDS*. American Society for Microbiology; 1994.
62 Beeching NJ, Fenech M, Houlihan CF. Ebola virus disease. *BMJ*. 2014;349:g7348.
63 Petersen LR, Jamieson DJ, Powers AM. Honein MAJNEJoM. *Zika Virus*. 2016;374(16):1552–1563.
64 Zhou P, Yang XL, Wang XG, Hu B, Zhang L, Zhang W, et al. A pneumonia outbreak associated with a new coronavirus of probable bat origin. *Nature*. 2020;579(7798):270–273.
65 Lam TT, Jia N, Zhang YW, et al. Identifying SARS-CoV-2-related coronaviruses in Malayan pangolins. *Nature*. 2020;583(7815):282–285.
66 Xiao K, Zhai J, Feng Y, et al. Isolation of SARS-CoV-2-related coronavirus from Malayan pangolins. *Nature*. 2020;583(7815):286–289.
67 Shi J, Wen Z, Zhong G, et al. Susceptibility of ferrets, cats, dogs, and other domesticated animals to SARS-coronavirus 2. *Science*. 2020;368(6494):1016–1020.
68 Huang C, Wang Y, Li X, et al. Clinical features of patients infected with 2019 novel coronavirus in Wuhan, China. *Lancet*. 2020;395 (10223):497–506.
69 Giorgi M, Cardarelli S, Ragusa F, et al. Phosphodiesterase inhibitors: could they be beneficial for the treatment of COVID-19? *Int J Mol Sci*. 2020;21(15).
70 Saleh J, Peyssonnaux C, Singh KK, Edeas M. Mitochondria and microbiota dysfunction in COVID-19 pathogenesis. *Mitochondrion*. 2020;54:1–7.
71 Csoka AB, Frost GI, Stern R. The six hyaluronidase-like genes in the human and mouse genomes. *Matrix Biol*. 2001;20(8):499–508.
72 Ding M, Zhang Q, Li Q, Wu T, Huang YZ. Correlation analysis of the severity and clinical prognosis of 32 cases of patients with COVID-19. *Respir Med*. 2020;167: 105981.
73 Turino GM, Cantor JO. Hyaluronan in respiratory injury and repair. *Am J Respir Crit Care Med*. 2003;167(9):1169–1175.
74 Bhattacharya J, Cruz T, Bhattacharya S, Bray BA. Hyaluronan affects extravascular water in lungs of unanesthetized rabbits. *J Appl Physiol*. 1989;66(6):2595–2599. (1985).
75 Qin C, Zhou L, Hu Z, et al. Dysregulation of immune response in patients with coronavirus 2019 (COVID-19) in Wuhan, China. *Clin Infect Dis*. 2020;71(15):762–768.
76 McKallip RJ, Do Y, Fisher MT, Robertson JL, Nagarkatti PS, Nagarkatti M. Role of CD44 in activation-induced cell death: CD44-deficient mice exhibit enhanced T cell response to conventional and superantigens. *Int Immunol*. 2002;14(9):1015–1026.
77 Kanse SM, Parahuleva M, Muhl L, Kemkes-Matthes B, Sedding D, Preissner KT. Factor VII-activating protease (FSAP): vascular functions and role in atherosclerosis. *Thromb Haemost*. 2008;99 (2):286–289.
78 Mambetsariev N, Mirzapoiazova T, Mambetsariev B, et al. Hyaluronic acid binding protein 2 is a novel regulator of vascular integrity. *Arterioscler Thromb Vasc Biol*. 2010;30(3):483–490.
79 Barrios-Lopez JM, Rego-Garcia I, Munoz Martinez C, et al. Ischaemic stroke and SARS-CoV-2 infection: a causal or incidental association? *Neurologia*. 2020;35(5):295–302.
80 Klein S, Cortese M, Winter SL, et al. SARS-CoV-2 structure and replication characterized by *in situ* cryo-electron tomography. *Nat Commun*. 2020;11(1):5885.
81 Burke JM, St Clair LA, Perera R, Parker R. SARS-CoV-2 infection triggers widespread host mRNA decay leading to an mRNA export block. *RNA*. 2021;27(11):1318–1329.
82 Mine S, Okada Y, Kawahara C, Tabata T, Tanaka Y. Serum hyaluronan concentration as a marker of angiopathy in patients with diabetes mellitus. *Endocr J*. 2006;53(6):761–766. advpub:0609110032-.
83 Kalay N, Elcik D, Canatan H, et al. Elevated plasma hyaluronan levels in pulmonary hypertension. *Tohoku J Exp Med*. 2013;230(1):7–11.